© 2016. Published by The Company of Biologists Ltd | Journal of Cell Science (2016) 129, 4509-4520 doi:10.1242/jcs.189142

RESEARCH ARTICLE

# RNA-dependent disassembly of nuclear bodies

**Yana R. Musinova[1,2], Olga M. Lisitsyna[1], Dmitry V. Sorokin[3,4], Eugene A. Arifulin[1], Tatiana A. Smirnova[5], Roman A. Zinovkin[1], Daria M. Potashnikova[5], Yegor S. Vassetzky[1,2,6] and Eugene V. Sheval[1,2,*]**

## ABSTRACT

Nuclear bodies are membraneless organelles that play important roles in genome functioning. A specific type of nuclear bodies known as interphase prenucleolar bodies (iPNBs) are formed in the nucleoplasm after hypotonic stress from partially disassembled nucleoli. iPNBs are then disassembled, and the nucleoli are reformed simultaneously. Here, we show that diffusion of B23 molecules (also known as nucleophosmin, NPM1) from iPNBs, but not fusion of iPNBs with the nucleoli, contributes to the transfer of B23 from iPNBs to the nucleoli. Maturation of pre-ribosomal RNAs (rRNAs) and the subsequent outflow of mature rRNAs from iPNBs led to the disassembly of iPNBs. We found that B23 transfer was dependent on the synthesis of pre-rRNA molecules in nucleoli; these pre-rRNA molecules interacted with B23 and led to its accumulation within nucleoli. The transfer of B23 between iPNBs and nucleoli was accomplished through a nucleoplasmic pool of B23, and increased nucleoplasmic B23 content retarded disassembly, whereas B23 depletion accelerated disassembly. Our results suggest that iPNB disassembly and nucleolus assembly might be coupled through RNA-dependent exchange of nucleolar proteins, creating a highly dynamic system with long-distance correlations between spatially distinct processes.

**KEY WORDS: Nuclear bodies, Nucleolus, Interphase prenucleolar body, Pre-rRNA, B23, NPM1, Self-organization**

## INTRODUCTION

The cell nucleus is a complex structure harboring a variety of discrete subnuclear organelles, collectively referred to as nuclear bodies. Nuclear bodies concentrate molecules to facilitate biological reactions, but unlike cytoplasmic organelles, nuclear bodies lack a defining membrane to separate them from the rest of the nucleus. Nuclear bodies are highly dynamic structures whose components can be rapidly exchanged with the surrounding nucleoplasm. Self-organization of nuclear bodies through transient protein–protein and/or protein–RNA interactions has been proposed (Misteli, 2001).

Nuclear body self-organization mechanisms have been intensively investigated in recent years, but whether nuclear body self-organization occurs stochastically or through an ordered, hierarchical process is not fully understood (Mao et al., 2011a; Dundr, 2012; Sleeman and Trinkle-Mulcahy, 2014). Immobilization of any component of Cajal bodies on chromatin is sufficient for the assembly of morphologically normal and apparently functional Cajal bodies, indicating that the biogenesis of Cajal bodies does not follow a hierarchical assembly pathway but instead follows a stochastic model (Kaiser et al., 2008). However, immobilization of individual paraspeckle proteins does not recruit other paraspeckle proteins or Men-ε/β long non-coding RNAs (also know as *NEAT1*), which are important structural components of paraspeckles (Mao et al., 2011b). By contrast, the sequential recruitment of proteins to histone locus bodies observed during development of the early *Drosophila* embryo supports the hypothesis of hierarchical assembly (White et al., 2011).

The models described above represent two extreme scenarios, but nuclear body assembly might include components of both assembly mechanisms. A compromised seeding model has been proposed in which a single component or a subset of components act hierarchically as seeds to initiate stochastic nuclear body growth (Dundr, 2011). Indeed, both coding and non-coding RNAs can nucleate the assembly of some nuclear bodies (Mao et al., 2011b; Shevtsov and Dundr, 2011; Chujo et al., 2015; Caudron-Herger et al., 2015), and it has been assumed that RNA molecules can seed the biogenesis of nuclear bodies. Proteins can also act as seeding molecules, as demonstrated for PML bodies (Kaiser et al., 2008; Mao et al., 2011a). Recently, phase separation of disordered proteins has been shown to lead to the formation of membraneless organelles (Hennig et al., 2015; Nott et al., 2015). Assembly of some nuclear bodies can also occur through a stepwise process due to the presence of several seeding components. For example, a short DNA sequence between the genes encoding histones H3 and H4 nucleates histone locus body assembly, but activity of the H3–H4 promoter is necessary to form mature histone locus bodies (Salzler et al., 2013).

Despite recent studies on the molecular mechanisms underlying the assembly and maintenance of several nuclear bodies, little is known about mechanisms of nuclear body disassembly. According to the stochastic self-organization model, both assembly and disassembly should be random, but in the hierarchical self-organization model, disassembly should follow the reverse order of assembly (Rajendra et al., 2010). Some experimental data agree with the latter supposition. Indeed, early pre-ribosomal RNAs (rRNA) processing proteins are released from prenucleolar bodies (PNBs) before late processing proteins during telophase disassembly of PNBs (Savino et al., 2001). Additionally, disassembly of mitotic interchromatin granules occurs at the final stages of mitosis, with each component being released and subsequently imported into daughter nuclei in a hierarchical order (Prasanth et al., 2003).

[1]A.N. Belozersky Institute of Physico-Chemical Biology, M.V. Lomonosov Moscow State University, Moscow 119992, Russia. [2]LIA1066 French-Russian Joint Cancer Research Laboratory, Villejuif 94805, France. [3]Centre for Biomedical Image Analysis, Faculty of Informatics, Masaryk University, Botanická 68a, Brno 602 00, Czech Republic. [4]Laboratory of Mathematical Methods of Image Processing, Faculty of Computational Mathematics and Cybernetics, M.V. Lomonosov Moscow State University, Moscow 119992, Russia. [5]Department of Cell Biology and Histology, Faculty of Biology, M.V. Lomonosov Moscow State University, Moscow 119992, Russia. [6]UMR8126, Université Paris-Sud, CNRS, Institut de cancérologie Gustave Roussy, Villejuif 94805, France.

*Author for correspondence (sheval_e@belozersky.msu.ru)

Y.R.M., 0000-0002-0790-5510; O.M.L., 0000-0003-4551-0154; D.V.S., 0000-0003-3299-2545; E.A.A., 0000-0002-3695-4215; T.A.S., 0000-0002-7575-8591; R.A.Z., 0000-0001-5337-4346; Y.S.V., 0000-0003-3101-7043; E.V.S., 0000-0003-1687-1321

**Received 12 March 2016; Accepted 2 November 2016**



Journal of Cell Science

Journal of Cell Science (2016) 129, 4509-4520 doi:10.1242/jcs.189142

RNA molecules nucleating the assembly of different nuclear bodies are more stably bound to nuclear bodies than proteins. Using single-particle tracking, 28S rRNA molecules have been shown to diffuse freely in the nucleoplasm, but their mobility is significantly reduced within nucleoli (Spille et al., 2015). Transcripts from one nucleolus organizer region within large nucleoli have been shown to occupy a distinct subnucleolar territory, also indicating that the rRNA molecules within nucleoli are not as mobile as nucleolar proteins (Grob et al., 2014). Fluorescence recovery after photobleaching (FRAP) analysis has revealed that the rate of Men-ε/β RNA exchange is significantly lower than that of paraspeckle proteins (Mao et al., 2011b).

Maintenance of nuclear bodies appears to require a constant influx of new RNA molecules because there is a constant outflow of molecules from the nuclear bodies. Indeed, when rRNA transcription is inhibited (i.e. rRNA molecule inflow is inhibited), the composition (Andersen et al., 2005) and structure (Shav-Tal et al., 2005) of nucleoli are strongly affected. Additionally, a similar effect has been recently illustrated for paraspeckles in living cells, where inhibition of transcription of Men-ε/β non-coding RNA led to disassembly of the structures, although the total Men-ε/β content was not reduced (Mao et al., 2011b). A reduction in the seeding molecule content might be one of the major mechanisms underlying nuclear body disassembly.

Some nuclear bodies are formed only transiently, including: (1) PNBs that form during telophase, whose proteins are gradually recruited to reforming nucleoli (Hernandez-Verdun, 2011); (2) interphase PNBs (iPNBs), which are nuclear bodies that form in the nucleoplasm during the reformation of nucleoli after disassembly under hypotonic conditions (Zatsepina et al., 1997); and (3) an embryonic variant of PNBs or 'extranucleolar droplets' (Korčeková et al., 2012; Berry et al., 2015). The disassembly of transient nuclear bodies occurs simultaneously with nucleolus assembly, and these spatially separated processes might be coupled by some unidentified mechanism.

We are interested in the overall dynamics of nuclear bodies (their assembly and disassembly). The iPNBs and nucleoli are one example of nuclear bodies that share common features such as both their formation and the maintenance of their integrity depending on the presence of nucleating RNA molecules. To detect iPNBs we used cells expressing nucleolar protein B23 fused to EGFP. B23, also known as nucleophosmin (NPM1), No38 or numatrin is a highly abundant nucleolar phosphoprotein with functions associated with ribosome biogenesis (Lindström, 2011), maintenance of genome stability (Lee et al., 2005; Amin et al., 2008; Koike et al., 2010; for a review, see Box et al., 2016), the nucleolar stress response (Avitabile et al., 2011), modulation of the p53 tumor suppressor pathway (Colombo et al., 2002; Bertwistle et al., 2004; Kurki et al., 2004), centrosome reduplication (Wang et al., 2005) and regulation of apoptosis (Ahn et al., 2005; Li and Hann, 2009). B23 is a member of the nucleoplasmin protein family, which includes the histone chaperones NPM2 and NPM3. B23 depletion is associated with disruption of nucleolar structure (Holmberg Olausson et al., 2015). These proteins share a conserved N-terminal oligomerization domain that mediates homopentamerization (Hingorani et al., 2000; Mitrea et al., 2014). B23 can bind nucleic acids (e.g. rRNA and DNA) through its C-terminal domain (Wang et al., 1994).

The results of the current work demonstrate that the main mechanism of transfer of material from iPNBs to nucleoli is diffusion of molecules between iPNBs and nucleoli. The transfer vector is dependent on two processes: (1) a decrease (outflow) in mature rRNA molecules in iPNBs, and (2) an increase (inflow) in newly synthesized pre-rRNA molecules in the nucleoli, which allows coupling of two spatially distinct macroscopic processes (iPNB disassembly and nucleolus assembly).

## RESULTS

### Dynamics of iPNB disassembly

Incubation of cultured HeLa cells expressing EGFP–B23 under hypotonic conditions (20% Hank's solution) and their subsequent return to an isotonic culture medium induced the formation of numerous nucleoplasmic B23-containing bodies (iPNBs) (Fig. S1). The quantity of iPNBs and their size changed during the reconstruction of nuclear organization under isotonic conditions (Fig. 1A). After the first 5 min of incubation under isotonic conditions, we observed the formation of numerous small (<0.2 µm) iPNBs that were uniformly distributed throughout the nucleoplasm. Between 5 and 30 min, the number of iPNBs gradually decreased, and the heterogeneity of iPNB size simultaneously increased, probably due to fusion of iPNBs with each other. The size of the largest iPNBs was ∼1 µm. The number and size of iPNBs in the cells slowly decreased between 30 min and 4 h.

To quantify this process, we measured the iPNB distribution density (number of iPNBs in a single optical section for the area of the nucleoplasm). The iPNB distribution density gradually decreased during the observation period (Fig. 1B). Simultaneously, we estimated the fraction of EGFP–B23 that accumulated in nucleoli, which could be roughly estimated by measuring the ratio of the integrated fluorescence intensity of nucleoli to the integrated fluorescence intensity of nuclei in a single optical section. Hypotonic treatment led to a substantial transfer of EGFP–B23 from nucleoli to the nucleoplasm (Fig. 1C). During incubation under isotonic conditions, the nucleolar fraction of EGFP–B23 gradually increased and reached the initial level after 4 h of recovery. These changes might be due either to selective EGFP–B23 proteolysis in the nucleoplasm or transfer of EGFP–B23 from iPNBs to nucleoli. We analyzed the EGFP–B23 content in cells during iPNB disassembly using immunoblotting with anti-B23 antibodies. The quantity of EGFP–B23, as well as that of endogenous B23, did not vary substantially during growth under isotonic conditions (Fig. 1D). We also analyzed the EGFP–B23 content using flow cytometry. The EGFP–B23 content observed based on the distribution of the fluorescence intensity was similar in control cells [5.896 arbitrary units (a.u.)] and cells that were incubated in hypotonic buffer and then in isotonic medium for 4 h (5.922 a.u.; Fig. 1E). Hence, we observed a bona fide transfer of nucleoplasmic EGFP–B23 from iPNBs to the nucleoli.

### Fusion of iPNBs with nucleoli is not a major mechanism of nucleolus reformation

EGFP–B23 transfer from the nucleoplasm to nucleoli might be a consequence of directed motion and fusion of iPNBs with nucleoli. To analyze iPNB motion, a time-lapse series of HeLa cells expressing EGFP–B23 was obtained with a confocal microscope; a total of 400 images from each cell were captured over 400 s. We did not detect any long-distance directed motions; the majority of iPNBs fluctuated rather stochastically within a relatively small volume of nuclear space (Fig. 2A; Movie 1).

We next verified whether iPNBs fused with nucleoli. The fusion of iPNBs with each other (Fig. 2B; Movie 2) and with nucleoli (Fig. 2C; Movie 3) was easily observed during the first hour after the return to isotonic medium. The frequency of fusion events between iPNBs rapidly declined during the first hour (Fig. 2D). The fusion of

Journal of Cell Science (2016) 129, 4509-4520 doi:10.1242/jcs.189142

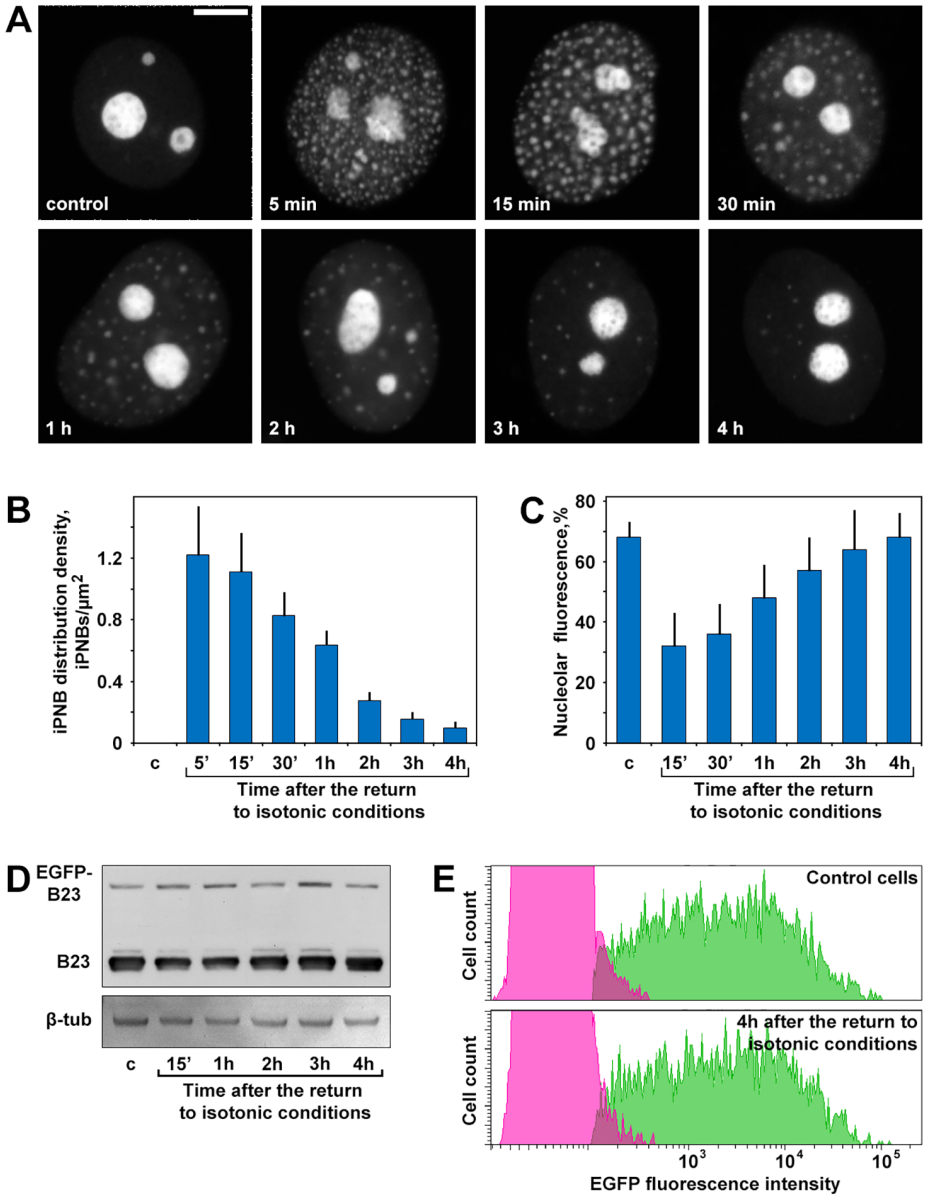


**Fig. 1. Dynamics of iPNB disassembly during recovery of HeLa cells from hypotonic stress.** (A) iPNBs were detected based on EGFP–B23 fluorescence in the control cells and in cells during recovery after hypotonic stress. Scale bar: 5 µm. (B) Estimation of the dynamics of iPNB numbers. The iPNB distribution density was calculated as the number of iPNBs in a single optical section acquired by the confocal microscope for the area of nucleoplasm. Results are mean±s.d. ($n$>20). (C) Estimation of EGFP–B23 content within nucleoli. Results are mean± s.d. ($n$>20). c, control cells. (D) Detection of EGFP–B23 and B23 using anti-B23 monoclonal antibodies in control cells (c) and in cells during recovery from hypotonic stress. β-tubulin (β-tub) was used as a loading control. (E) EGFP–B23 fluorescence analysis by flow cytometry in HeLa cells under control conditions and 4 h after hypotonic stress, showing that the EGFP-positive cell populations remained unchanged. The images are representative of three independent measurements. Right cell population (green), EGFP–B23-expressing cells; left cell population (magenta), EGFP–B23-negative cells.

iPNBs with nucleoli was an infrequent event and mainly occurred during the first 20 min after recovery from hypotonic shock. Taken together, our data indicate that iPNBs are predominantly constrained in their mobility, and the infrequent fusion of iPNBs with nucleoli does not lead to massive transfer of nucleolar material from the nucleoplasm to nucleoli.

### EGFP–B23 is transferred from iPNBs to nucleoli by diffusion

Because iPNB fusions with nucleoli only led to limited and short-term transfer of EGFP–B23 to nucleoli, we used live-cell imaging to examine the possibility that EGFP–B23 was transferred to nucleoli through iPNB-directed motions during the late stages of nucleolar reformation. We analyzed stacks of confocal sections from each time point (4D microscopy) to exclude the loss of iPNB tracks due to movements in 3D space. The iPNBs exhibited low mobility, and directed iPNB movement was not observed, with only rare fusion events being recorded (Fig. 3A; Movie 4). At the same time, the fluorescence intensity of individual iPNBs gradually decreased, indicating that EGFP–B23 was removed from iPNBs (Fig. 3B). To quantify this process, we measured the fluorescence intensity of total nuclei as well as the intensity of nucleoli and iPNBs in projections after correction for photobleaching (Fig. 3C). The fluorescence intensity of iPNBs was gradually decreased, and the fluorescence intensity of nucleoli was simultaneously increased, indicating that EGFP–B23 might be transferred from iPNBs to the nucleoli by diffusion.

Transfer by diffusion is possible only if EGFP–B23 is freely exchanged between iPNBs and the surrounding nucleoplasm. The dynamics of EGFP–B23 were investigated using fluorescence recovery after photobleaching (FRAP). The half-time of fluorescence recovery was ~3.6 s in iPNBs and ~6.6 s in nucleoli, indicating that EGFP–B23 was quickly exchanged between iPNBs and the nucleoplasm, and nucleoli and nucleoplasm (Fig. 3D). It should be noted that the half-time of fluorescence recovery for EGFP–B23 within the nucleoli of control cells was slightly greater ($t_{1/2}$≈8.1 s; Fig. 3E). Thus, EGFP–B23 is more mobile in cells during their recovery from hypotonic shock, and diffusion appears to be an important mechanism of EGFP–B23 transfer from iPNBs to nucleoli.

Journal of Cell Science (2016) 129, 4509-4520 doi:10.1242/jcs.189142

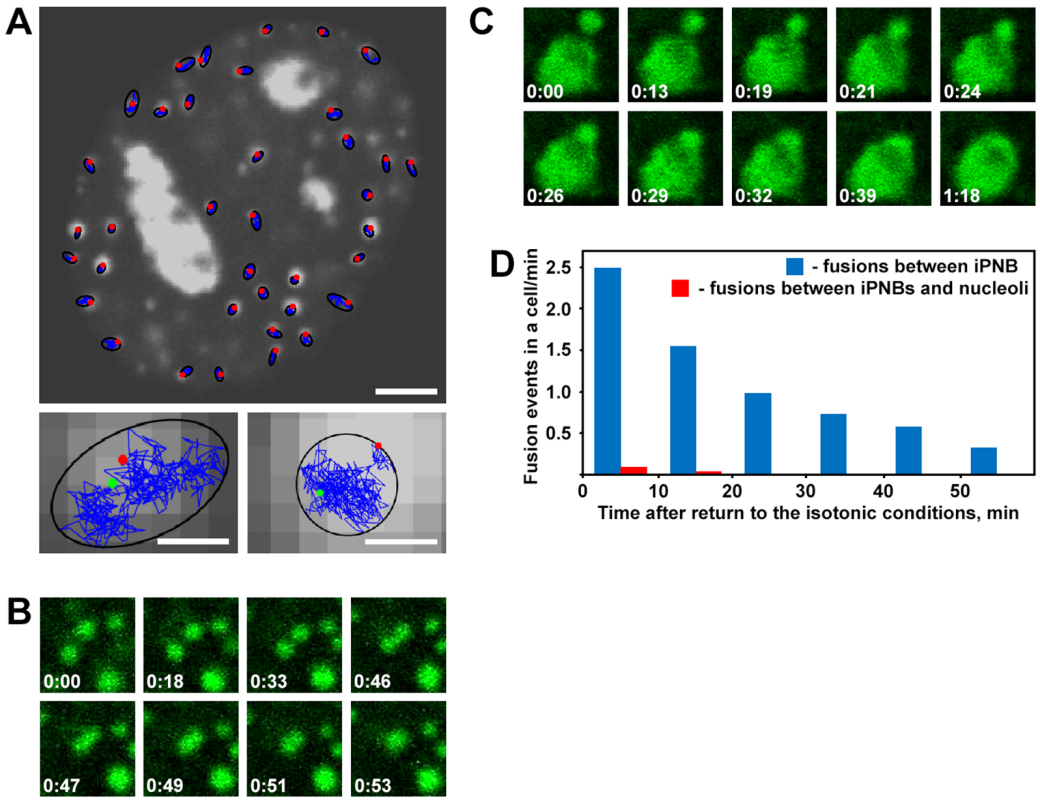


**Fig. 2. Tracking analysis of iPNBs during recovery of HeLa cells from hypotonic treatment.** (A) Localized movement of iPNB bodies (top panel) and enlarged examples of individual iPNB tracks (bottom panels). The tracks of iPNBs (blue) were plotted over the first frame of the sequence. Red and green dots represent the beginning and the end of the trajectory, respectively. Scale bars: 5 µm (top panel); 0.1 µm (bottom panels). (B) An example of fusion of two iPNBs with each other (live-cell imaging). (C) An example of fusion of iPNBs with the nucleolus. Because the nucleoli were not marked separately to the iPNBs, we selected the largest EGFP–B23-containing bodies as possible nucleoli. (D) The frequencies of iPNB fusion events with each other and with nucleoli at different times after the return to isotonic conditions.

iPNBs have been described as nuclear bodies whose structure and behavior are extremely similar to the PNBs of telophase cells (Zatsepina et al., 1997). Here, we have compared the crucial features of iPNB and PNB disassembly. For this purpose, we acquired and analyzed stacks of confocal sections of telophase cells. The PNBs (similar to iPNBs) exhibited low mobility, and directed PNB movements were not observed (Fig. S2A,B). The fluorescence intensity of individual PNBs gradually decreased (Fig. S2C).

### iPNBs are assembled around RNAs

We next investigated the possible role of RNAs in the maintenance and disassembly of iPNBs. Using the RNA-specific stain SYTO RNASelect, we detected the presence of RNA molecules within iPNBs (Fig. 4A). To ascertain the time of synthesis of these RNA molecules, we co-transcriptionally labeled RNA molecules using 5-ethynyl uridine. After a short (10 min) incubation with ethynyl uridine, no incorporation of ethynyl uridine within iPNBs was observed (Fig. 4B), indicating that RNA molecules accumulated, but were not synthesized within iPNBs. We next investigated whether these RNA molecules were synthesized before hypotonic treatment and accumulated in iPNBs during their assembly by preincubating cells with ethynyl uridine for 2 h before hypotonic treatment. Labeled RNA molecules were detected within iPNBs, indicating that they were indeed synthesized before hypotonic treatment (Fig. 4C). We then analyzed whether some RNA molecules could be synthesized in nucleoli after the return to isotonic medium and then transferred to iPNBs and accumulate within them. Ethynyl uridine was incorporated into cellular RNAs during 2 h of growth in isotonic medium after hypotonic treatment, but in this case, no labeled RNA molecules were detected within iPNBs (Fig. 4D). Thus, RNAs detected within iPNBs were synthesized before hypotonic treatment, and there was no inflow of *de-novo*-synthesized RNA molecules to the iPNBs after the return to isotonic medium. When HeLa cells were incubated with 20 µg/ml actinomycin D (ActD) for 4 h before hypotonic treatment to block rRNA transcription, iPNB assembly after hypotonic shock was significantly inhibited (Fig. S3). Because treatment with 10 µg/ml α-amanitin, which inhibits both RNA polymerase II and III transcription, did not significantly influence iPNB disassembly (Fig. S3), it appears that rRNA plays a seeding role during their formation.

### iPNB disassembly is linked to pre-RNA processing

Through fluorescence *in situ* hybridization (FISH) with probes specific for 28S rRNA, we demonstrated that iPNBs contained rRNA molecules (Fig. 5A). Pre-rRNA processing was shown to occur within the PNBs of telophase cells (Carron et al., 2012). To determine whether pre-rRNAs were processed in iPNBs, we employed the FISH technique, which was carried out using a combination of eight probes complementary to different segments of the transcribed spacers or mature rRNA to discriminate between early and late precursors (Fig. 5B). No labeling within the iPNBs was observed using the probe specific for the 5′-ETS leader sequence (ETS1-297) or the 5′-ETS-specific probe (ETS1-1399), indicating that pre-rRNA within iPNBs had already undergone cleavage at sites A′ and A0 (data not shown). Probes ETS1-18S and ITS1-160 labeled iPNBs up to 1 h after the

Journal of Cell Science (2016) 129, 4509-4520 doi:10.1242/jcs.189142

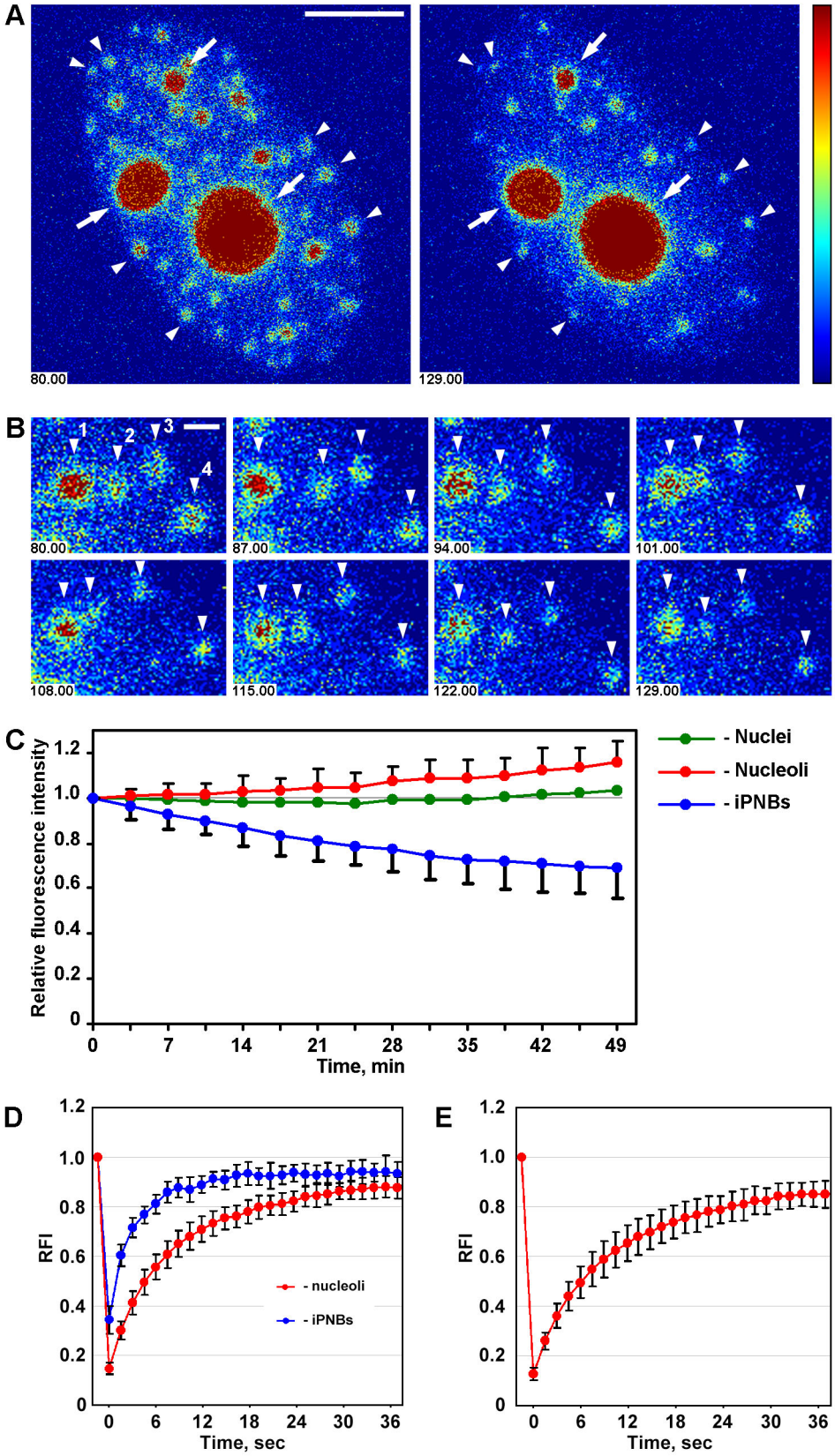


**Fig. 3. Analysis of EGFP–B23 transfer from iPNBs to nucleoli during recovery of HeLa cells from hypotonic stress.** (A) Average projections of the image stacks show low mobility of iPNBs and a gradual decrease in the EGFP–B23 content in individual iPNBs (indicated by arrowheads). Time is displayed in min:s from the time of the return to isotonic conditions. Nucleoli are indicated with arrows. Scale bar: 5 µm. (B) Magnified views of the nucleoplasm of EGFP–B23-expressing cells. iPNB brightness gradually decreased over the observation time. iPNBs are indicated with arrowheads. The iPNBs marked as 1 and 2 moved toward each other and nearly fused at 101–108 min but then moved in different directions, indicating an absence of directed iPNB movement toward each other. Scale bar: 1 µm. (C) Relative fluorescence intensity of the nuclei, nucleoli and iPNBs. Results are mean±s.d. ($n$=10). (D) FRAP analysis of EGFP–B23 mobility in iPNBs and nucleoli after the return to isotonic conditions (the movies were acquired during the interval from 20 to 40 min after the return to isotonic culture medium). Results are mean±s.d. ($n$=12 and 18). (E) FRAP analysis of EGFP–B23 mobility in nucleoli in the control cells. Results are mean±s.d. ($n$=14).

return of cells to isotonic medium, but not thereafter (Fig. 5C). The 5′ ITS1 probe and the probe for 18S rRNA labeled iPNBs for 1–2 h after the return to isotonic medium, but not thereafter, indicating that after that time, 18S rRNA was exported from the iPNBs. By contrast, the 5.8S-ITS2 and 28S rRNA probes labeled iPNBs for up to 4 h after the return to isotonic conditions. It should be noted that the labeling with FISH probes was visible within all iPNBs. The observed intensity of iPNB labeling with 5.8S-ITS2 and 28S rRNA probes gradually

Journal of Cell Science (2016) 129, 4509-4520 doi:10.1242/jcs.189142

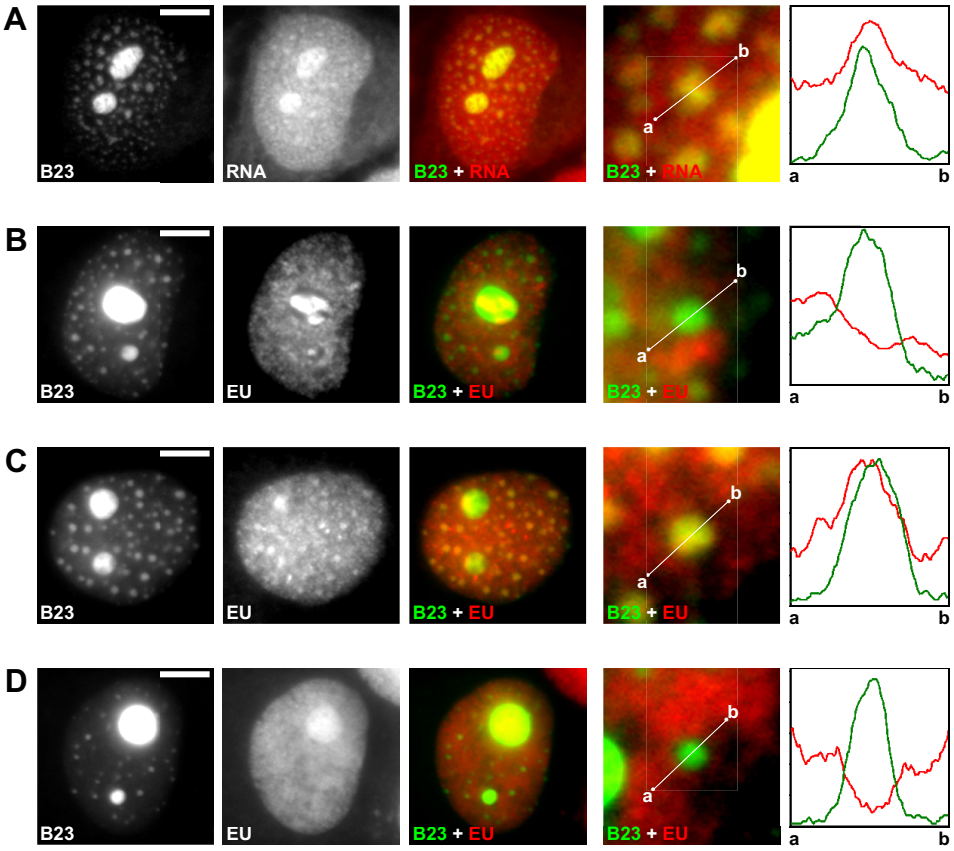


**Fig. 4. iPNBs in HeLa cells during recovery from the hypotonic treatment contain RNA molecules.** (A) iPNBs contain RNA (stained with the RNA-specific stain SYTO RNASelect). (B) RNA within iPNBs was not labeled after a brief (10 min) incubation with ethynyl uridine (EU), indicating the absence of RNA synthesis within iPNBs. (C) iPNB RNAs were synthesized before hypotonic treatment. RNA within iPNBs was labeled when ethynyl uridine was incorporated in cellular RNA for 2 h before hypotonic treatment. (D) RNAs synthesized after the return to isotonic conditions were not included in iPNBs. RNA within iPNBs was not labeled when ethynyl uridine was incorporated in cellular RNA for 2 h after hypotonic treatment. The images on the right-hand side show the fluorescence intensity along the indicated line. Scale bars: 5 µm.

decreased during incubation in isotonic medium, and the typical exposure times for cells at 4 h after the return to isotonic conditions were approximately two- to three-fold longer than those used for cells at 15 min after the return to isotonic conditions, indicating a gradual departure of mature rRNA molecules from iPNBs.

The gradual and consecutive disappearance of rRNA precursor molecules from iPNBs indicates that pre-rRNA processing indeed occurs within iPNBs. Many non-ribosomal factors involved in pre-rRNA processing and ribosome biogenesis fall into different families of energy-consuming enzymes (Kressler et al., 2010); therefore, we used an ATP depletion treatment to analyze iPNB disassembly. We observed that the iPNB distribution density was not substantially reduced, even after 4 h of growth in buffer containing sodium azide and 2-deoxy-D-glucose, in contrast to the control (Fig. 6A,B). The process of pre-rRNA processing upon ATP depletion was analyzed using FISH. All hybridization probes, except for ETS1-297 and ETS1-1399, labeled iPNBs in cells even after 4 h of growth in isotonic medium, indicating that pre-rRNA processing in these cells was inhibited (Fig. 6C).

A recent study has shown that some proteins might be immobilized within nucleoli after a heat shock or acidic and transcriptional stresses on specific non-coding RNAs originating from the ribosomal intergenic spacer (Audas et al., 2012). Using FRAP, we demonstrated that after ATP depletion, EGFP–B23 in iPNBs was only slightly less mobile than in the iPNBs of control cells (Fig. 6D), and the stabilization of iPNB organization was therefore not induced by B23 immobilization. Thus, our data indicate that inhibition of pre-rRNA processing appears to play an important role in iPNB stabilization.

### B23 transfer to reforming nucleoli affects iPNB disassembly

Our results agree with the idea that pre-rRNA molecules play a seeding role in iPNB maintenance, and the removal of mature rRNA molecules leads to gradual iPNB disassembly. Taking the high mobility of EGFP–B23 into consideration, the removal of this protein from iPNBs might be dependent on the presence of pre-rRNA within nucleoli. The recovery of rRNA transcription during the restoration of nuclear organization after hypotonic shock leads to accumulation of newly synthesized pre-rRNAs in nucleoli and dynamic accumulation of EGFP–B23 in nucleoli. We next blocked rRNA transcription by incubating cells in isotonic medium containing 0.1 µg/ml ActD after hypotonic treatment. The iPNB distribution density in these cells gradually decreased during incubation, but the decrease was slightly slower as compared with that in control cells (Fig. 7A). The iPNBs in cells after 4 h of incubation in the presence of ActD were both more numerous and larger than the iPNBs of control cells. By contrast, the nucleoli were small, and a substantial amount of EGFP–B23 was distributed throughout the nucleoplasm. Estimation of EGFP–B23 fluorescence in the nucleoli and nucleoplasm demonstrated that in control cells, the fraction of nucleoplasmic EGFP–B23 gradually decreased, whereas in ActD-treated cells, it gradually increased (Fig. 7B). EGFP–B23, which was removed from the iPNBs, appeared to accumulate in the nucleoplasm.

After 4 h of incubation in the presence of ActD, the iPNBs were only labeled with 5.8S-ITS2 and 28S rRNA probes, similar to for control cells (Fig. 7C), and thus, RNA FISH did not allow us to detect inhibition of pre-rRNA processing in ActD-treated cells. However, the intensity of labeling with these two probes was visibly higher than in the control cells. Thus, mature rRNAs remained inside iPNBs. The possibility that ActD treatment led to defects in the nuclear export of pre-ribosomes or that the excess of B23 in the nucleoplasm might have led to this effect cannot be excluded. If the latter alternative is true, B23 depletion could influence iPNB disassembly. Therefore, we analyzed iPNB dynamics in B23-

Journal of Cell Science (2016) 129, 4509-4520 doi:10.1242/jcs.189142

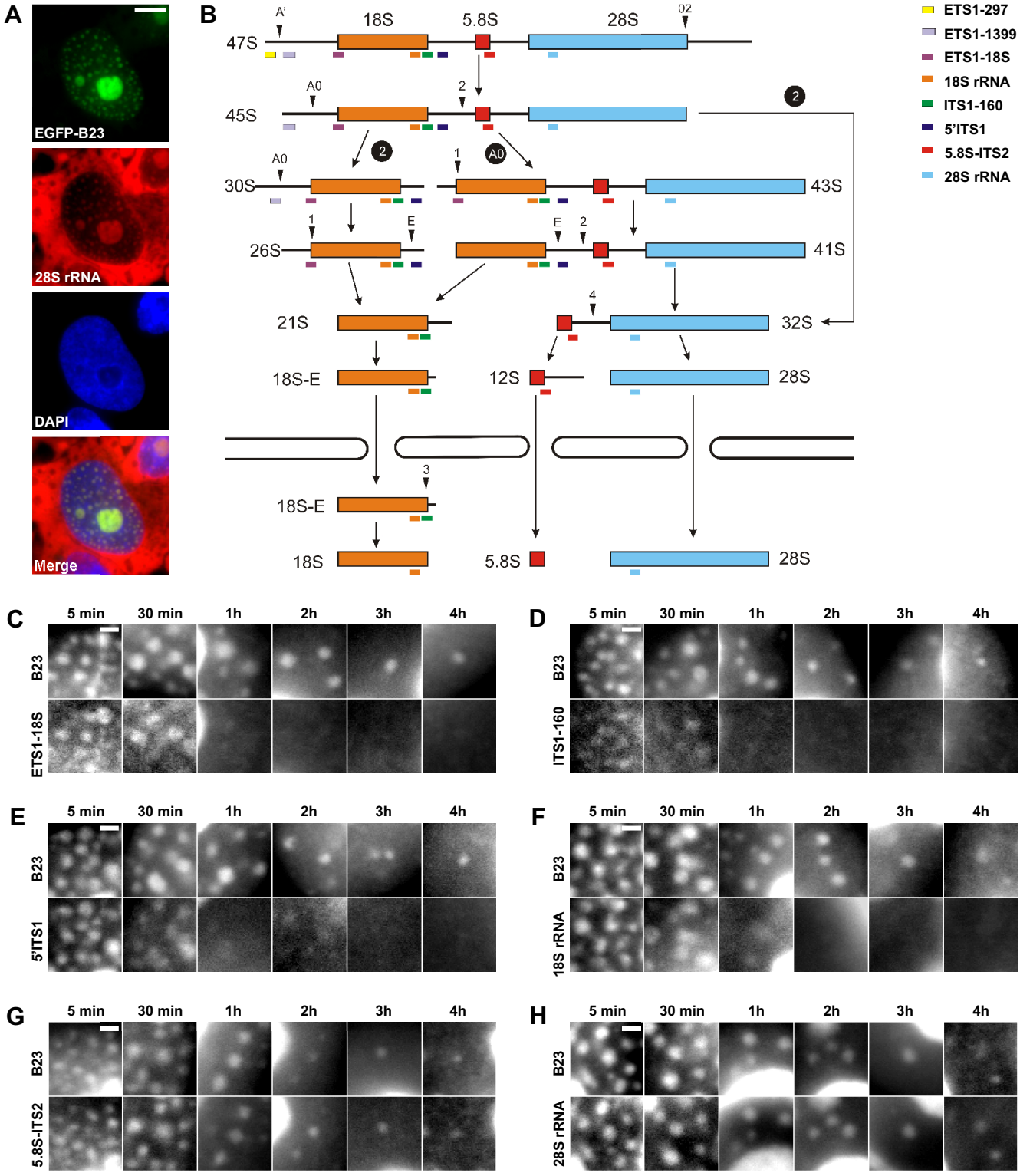


**Fig. 5. Maturation of pre-rRNA within iPNBs in HeLa cells during recovery after hypotonic treatment.** (A) iPNBs contain 28S RNA at 30 min after the return to isotonic conditions. (B) Pre-rRNA processing pathways in human cells (modified from Henras et al., 2014). The probes used to detect the pre-rRNAs in FISH experiments are drawn as colored boxes. This figure panel is published under a Creative Commons BY-NC license (https://creativecommons.org/licenses/by-nc/4.0/). (C–H) Localization of different pre-rRNAs within EGFP–B23-containing iPNBs at the indicated time after return to isotonic conditions. The cropped regions (4 µm×4 µm) are presented. Scale bars: 5 µm (A); 1 µm (C–H).

depleted cells. We generated lentivirus constructs for expression of short hairpin RNA (shRNAs) to stably deplete B23 and obtained clones of HeLa cells expressing either control or B23 shRNA. The amount of B23 in cells expressing B23 shRNA was substantially decreased (Fig. 7D,E). To detect iPNBs in these experiments, we used either 28S rRNA probes (Fig. 7F) or anti-B23 antibodies (B23 was substantially depleted, but a residual amount was sufficient to identify B23 localization using the monoclonal antibodies; the

Journal of Cell Science (2016) 129, 4509-4520 doi:10.1242/jcs.189142

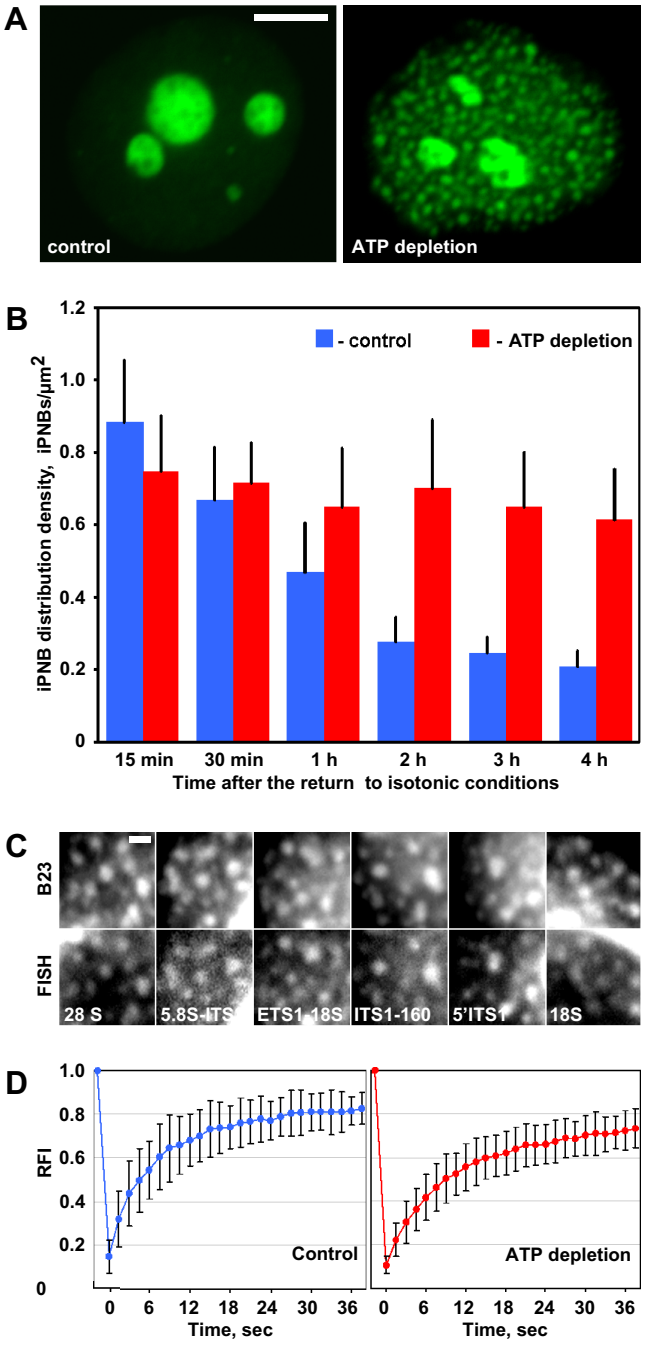


**Fig. 6. ATP depletion inhibits pre-rRNA processing and blocks iPNB disassembly.** (A) Representative images of nuclei from cells incubated after hypotonic stress in the culture medium (control) or Medium 1 (see Materials and Methods) containing sodium azide and deoxyglucose for 4 h (ATP depletion). After ATP depletion, the nucleoplasm contained numerous iPNBs. (B) Estimation of the iPNB distribution density during the reformation of nuclear organization in control cells and in cells grown in the presence of sodium azide and deoxyglucose. Results are mean±s.d. ($n$>20). (C) FISH analysis demonstrated that iPNBs in cells grown in the presence of sodium azide and deoxyglucose contained pre-rRNA, indicating that pre-rRNA processing in these cells was inhibited. (D) FRAP analysis of EGFP–B23 mobility in the iPNBs of control cells (left panel) and the iPNBs of cells grown in a solution containing sodium azide and deoxyglucose (right panel). Results are mean±s.d. ($n$=12 and 14). Scale bars: 5 μm (A); 1 μm (C).

conditions of the image acquisition were selected in such a way that the brightness of the final images was similar, independently of the level of B23 expression; data not shown). The iPNBs in B23-depleted cells were easily detected using both methods early after recovery from hypotonic shock (5–30 min) but were not visible after 1 h of incubation, indicating that the iPNBs in these cells were disassembled substantially more rapidly than in cells expressing the control shRNA.

It can be assumed that B23 depletion might lead to accelerated maturation or degradation of pre-rRNAs. To examine this hypothesis, quantitative real-time PCR (qRT-PCR) was carried out. The ratio of 47S-30S pre-rRNA to 47S-12S pre-rRNA was estimated. If B23 depletion induces increased maturation, a decrease in this ratio would be detected. However, this was not the case, and a slight increase in the content of 47S-30S pre-rRNA (i.e. early forms of pre-rRNA) was detected in B23-depleted cells, especially after the return to isotonic conditions (Fig. S4A), indicating that pre-rRNA processing was either unchanged or even slightly inhibited. Hence, acceleration of iPNB disassembly in B23-depleted cells was not due to accelerated maturation or degradation of pre-rRNAs. Importantly, RNA FISH demonstrated that immature pre-rRNAs were detectable in the nucleoplasm and cytoplasm of B23-depleted cells (Fig. S4B), indicating that the acceleration of iPNB disassembly was due to increased export of pre-ribosomes (including immature pre-ribosomes, which were not exported in control cells), rather than to modified pre-rRNA processing. Thus, we propose that B23 content also affects iPNB disassembly and the nuclear export of pre-mRNA, although further studies are required to confirm this hypothesis.

## DISCUSSION

PNBs in telophase cells are the best-known type of transient nuclear bodies, and their disassembly might be coupled with the reformation of nucleoli after mitosis. iPNBs are formed after the return of cultured cells to isotonic conditions following hypotonic stress, and they appear to be involved in the reformation of nucleolar organization (Zatsepina et al., 1997). The iPNB model is convenient for microscopic and biochemical studies because iPNB disassembly occurs synchronously in all interphase cells, and as shown in our experiments, the process of iPNB disassembly occurs much more slowly than the process of telophase PNB disassembly. Indeed, PNBs containing the late pre-rRNA processing protein Nop52 (also known as RRP1) can be observed for 80 min ± 20 min (Savino et al., 2001), whereas iPNBs are visible up to 4 h after the return to isotonic medium. iPNBs are similar in many respects to telophase PNBs (Zatsepina et al., 1997), but they are a distinct type of nuclear bodies with specific properties. Here, we used iPNBs to study the coupling between the disassembly of transient nuclear bodies and the assembly of nucleoli.

First, we tested the hypothesis that iPNBs might exhibit movement and transfer nucleolar material. Fusion with nucleoli occurred only at early times of recovery from hypotonic stress and did not contribute substantially to the reconstitution of nucleoli. We next demonstrated that EGFP–B23 was transferred to nucleoli through diffusion, which is supported by: (1) the lack of directional movement of iPNBs to the nucleoli, (2) the gradual decrease in EGFP–B23 in the iPNBs and parallel increase in EGFP–B23 in nucleoli, and (3) the constant exchange of EGFP–B23 between iPNBs and the surrounding nucleoplasm. A similar pattern of disassembly is typical of telophase cells: low mobility of PNBs and a gradual decrease in EGFP–B23 in PNBs were observed through live-cell imaging of telophase cells. Similar results were obtained previously. For example, as the cells progress through telophase, the fibrillarin–GFP fluorescence from PNBs decreases, with a concomitant increase in the intensity of nucleolar fluorescence

Journal of Cell Science (2016) 129, 4509-4520 doi:10.1242/jcs.189142

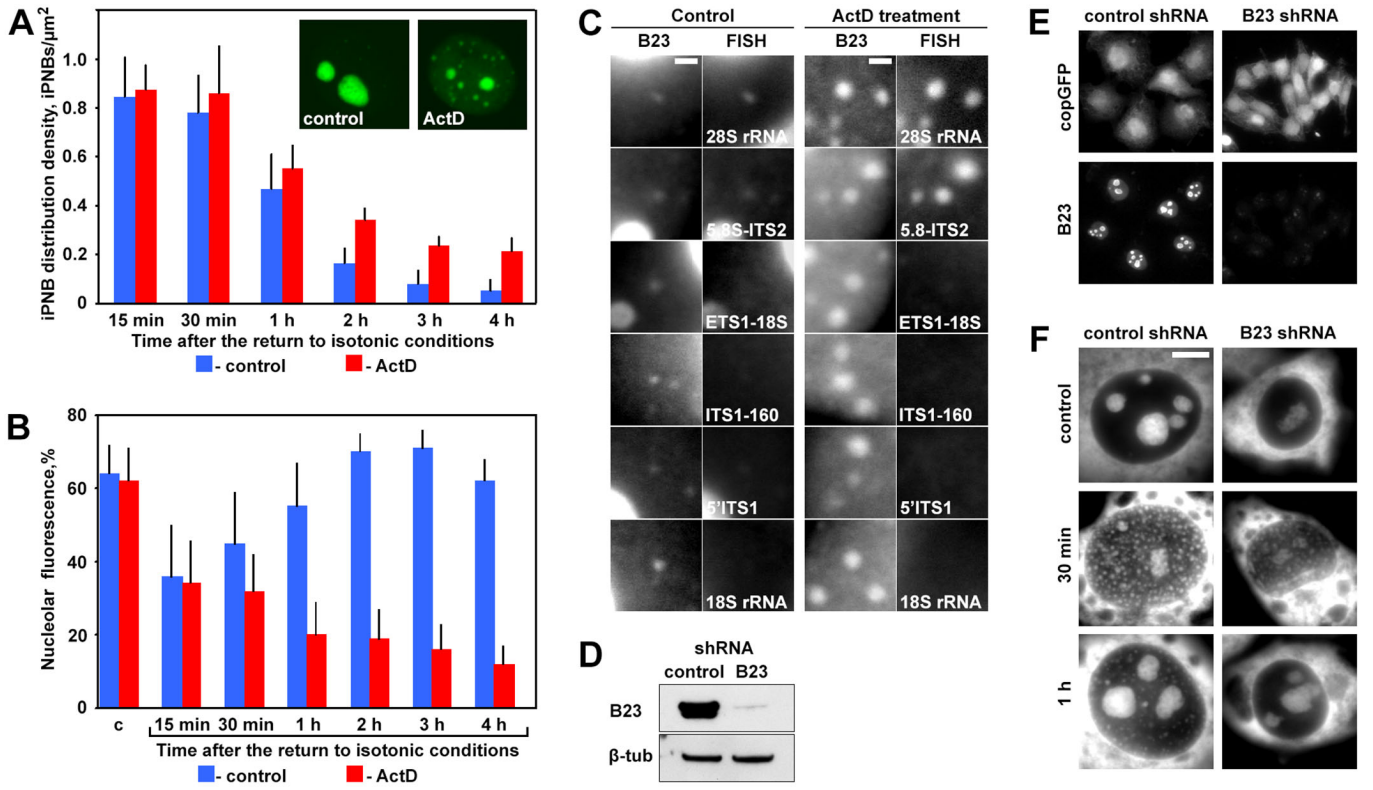


**Fig. 7. iPNB disassembly during recovery of HeLa cells from hypotonic treatment depends on the nucleoplasmic B23 concentration.** (A) Disassembly of iPNBs was delayed in cells incubated in the presence of ActD. Results are mean±s.d. ($n$>20). The images show the localization of EGFP–B23 in control and ActD-treated cells at 4 h after the return to isotonic culture medium. (B) Estimation of EGFP–B23 content within the nucleoli of control cells and cells grown in the presence of ActD. Results are mean±s.d. ($n$>20). (C) FISH analysis demonstrated that iPNBs in cells grown for 4 h in the presence of ActD contained only mature 28S and 5.8S rRNA, but not pre-rRNAs, similar to control cells. Thus, pre-mRNA processing was not inhibited by ActD treatment. (D) Detection of B23 content in cells expressing control shRNA and B23 shRNA. β-tubulin (β-tub) was used as a loading control. (E) Immunofluorescence detection of B23 content within cells expressing control shRNA and B23 shRNA. The cells were observed under identical conditions, and the images were processed similarly. (F) iPNBs in the control and B23 shRNA-expressing cells (FISH with a probe for 28S rRNA). At 30 min after the return to isotonic conditions, iPNBs were visible in both cell types. At 1 h, iPNBs were observed only in cells expressing the control shRNA. Scale bars: 1 μm (C); 5 μm (F).

(Dundr et al., 2000). Fibrillarin–GFP exchange between PNBs and the nucleoplasm in telophase cells has been demonstrated through FRAP analysis (Dundr et al., 2000), and B23 exchange between PNBs and nucleoli has been demonstrated using photoactivatable fluorescent proteins (Muro et al., 2010).

Diffusion leads to microscopically visible transfer of EGFP–B23 from iPNBs to nucleoli. In free exchange situations, the transfer of proteins is dependent on alterations in the number of protein-binding sites within different structures, and the removal of proteins can be driven by decreasing the number of binding sites within iPNBs. RNA molecules play a crucial role in the maintenance of some nuclear bodies, and RNA transcripts are able to nucleate nuclear body assembly (Mao et al., 2011b; Shevtsov and Dundr, 2011). Nuclear body maintenance requires a constant influx of new RNA molecules because there is a constant outflow of molecules from nuclear bodies. This effect has been elegantly illustrated for paraspeckles, where inhibition of Men-ε/β non-coding RNA transcription leads to the disassembly of these nuclear bodies, even when the total Men-ε/β level is not reduced (Mao et al., 2011b). Inhibition of rRNA transcription also leads to nucleolus reorganization and disassembly (Shav-Tal et al., 2005). We have shown here that there is no influx of newly synthesized rRNA molecules into iPNBs. Pre-rRNA processing occurs within iPNBs, and the amount of pre-RNA and mature rRNA gradually decreases. It appears that the processing and outflow of mature rRNA molecules play a crucial role in the disassembly of iPNBs. These data are in agreement with the results of O'Donahue and colleagues (Carron et al., 2012), who demonstrated that pre-rRNA processing occurred within PNBs. Hence, the disassembly mechanisms of both types of nuclear bodies are dependent on the outflow of RNA molecules.

We propose that iPNB disassembly is dependent on both the outflow of RNA molecules from these nuclear bodies and the increase in the RNA concentration in nucleoli due to the restoration of rRNA transcription. Indeed, inhibition of pre-rRNA transcription with ActD retarded iPNB disassembly, although pre-rRNA processing was not substantially altered. These results are in agreement with the data of Roussel and colleagues, who demonstrated that processing of pre-rRNA is not sufficient to induce disappearance of PNBs, which appears to require the presence of functional nucleoli (Sirri et al., 2016). Further studies are necessary to confirm our hypothesis.

This long-distance correlation between processes within nucleoli and iPNBs probably occurs through the nucleoplasmic pool of B23. ActD treatment led to an excess concentration of B23 in the nucleoplasm, and it appears that this excess of B23 molecules retarded iPNB disassembly, possibly due to retention of mature rRNA in iPNBs. By contrast, in B23-depleted cells, iPNB

Journal of Cell Science (2016) 129, 4509-4520 doi:10.1242/jcs.189142

disassembly occurred more quickly than in the control cells. A similar relationship between nucleolus size and the nucleolar protein concentration has been described recently (Weber and Brangwynne, 2015).

Thus, we show that diffusion of B23 molecules from iPNBs to nucleoli, but not fusion of iPNBs with nucleoli, contributes to the transfer of B23 from iPNBs to the nucleoli. Protein diffusion is a non-directional process, but B23 appears to be transferred from iPNBs to nucleoli in an orderly manner. The transfer vector is dependent on two processes: (1) a decrease (outflow) in mature rRNA molecules in iPNBs, and (2) an increase (inflow) in newly synthesized pre-rRNA molecules in nucleoli. This couples the two spatially distinct macroscopic processes of iPNB disassembly and nucleolus assembly, creating an integrated system with long-distance correlations. As many nuclear bodies contain RNA, similar principles might apply to their functioning in cells. Determining this will be the object of our further work.

## MATERIALS AND METHODS

### Cell culture and induction of iPNB formation

HeLa cells (Russian Cell Culture Collection, Institute of Cytology of the Russian Academy of Sciences, Saint Petersburg) were grown in Dulbecco's modified Eagle's medium supplemented with L-glutamine, 10% fetal calf serum (HyClone) and an antibiotic and antimycotic solution (Sigma). To induce interphase prenucleolar body formation, the cells were incubated in 20% Hank's balanced salt solution for 15 min and then transferred to complete culture medium (Zatsepina et al., 1997). To inhibit RNA transcription, the cells were grown in medium with 0.1 µg/ml ActD. ATP depletion was carried out as described by Bhattacharya et al. (2006). Briefly, the cells were treated with 20% Hank's solution for 15 min and then transferred to Medium 1 (150 mM NaCl, 5 mM KCl, 1 mM $CaCl_2$, 1 mM $MgCl_2$, 20 mM HEPES, pH 7.4) containing 10 mM sodium azide and 6 mM 2-deoxy-D-glucose. We used either anti-B23 antibodies or EGFP–B23-expressing plasmid for iPNB detection. A higher concentration of an antigen within the nucleoli might prevent its proper recognition by specific antibodies (Sheval et al., 2005; Svistunova et al., 2012); therefore, the EGFP–B23-expressing plasmid was used in the majority of our experiments, with the exception of the experiments involving shRNAs. The EGFP–B23 plasmid was a gift from Xin Wang (Addgene plasmid no. 17578) (Wang et al., 2005). Cellular transfection was performed using the Lipofectamine 2000 reagent (Invitrogen) according to the manufacturer's instructions. For iPNB quantification, we acquired images of fixed cells expressing EGFP–B23 using an LSM 510 confocal microscope and measured a number of iPNBs in a single optical section for the area of the nucleoplasm (iPNB distribution density).

### Immunoblotting and immunocytochemistry

For immunoblotting, the cells were lysed in Laemmli sample buffer, boiled for 3 min and resolved on a 12.5% SDS-polyacrylamide gel. The proteins were transferred to a nitrocellulose membrane using the Trans-Blot Turbo Transfer System (Bio-Rad). These membranes were blocked in 1% bovine serum albumin and incubated with primary antibodies. Monoclonal antibodies against B23 (1:5000; cat. no. B0556, Sigma) and β-tubulin (1:5000; cat. no. T0198, Sigma) were used. The membranes were washed in PBS and then incubated with a secondary horseradish-peroxidase-conjugated antibody (1:18,000; Sigma). The antibody-bound proteins were detected using the Pierce ECL western blotting substrate (Life Technologies).

For immunofluorescent labeling, the cells were fixed in 3.7% formaldehyde at room temperature for 15 min and subsequently permeabilized with 0.5% Triton X-100 in PBS for 5 min. After washing in PBS, the cells were incubated in 1% BSA for 45 min, then incubated with anti-B23 antibodies (1:200; cat. no. B0556, Sigma) for 60 min, washed again, and incubated with Alexa-Fluor-555-conjugated antibodies (1:700; Invitrogen) for 45 min. Finally, the cells were washed again, stained with a 0.1 µg/ml solution of DAPI (Sigma) and embedded in Mowiol (Calbiochem) containing an anti-bleaching agent (DABCO, Sigma). The preparations were observed using an Axiovert 200M microscope (Carl Zeiss) equipped with an ORCAII-ERG2 cooled CCD camera (Hamamatsu).

The localization of RNA was analyzed using the SYTO RNASelect Green Fluorescent Cell Stain (Invitrogen) according to the manufacturer's instructions. Briefly, cells were fixed in pre-chilled methanol at −20°C for 10 min, then washed in PBS and stained with a 500 nM solution of the RNASelect stain for 20 min at room temperature. After washing in PBS, the cells were counterstained with DAPI and mounted in Mowiol.

Additionally, co-transcriptional labeling of RNA molecules using 5-ethynyl uridine (Invitrogen) was performed, for which the cells were incubated in culture medium containing 1 mM ethynyl uridine (the duration of the incubations is indicated in the Results section). For the detection of incorporated ethynyl uridine, the Click-iT EdU Alexa Fluor 555 Imaging Kit was used (Invitrogen) according to the manufacturer's instructions. Incubation in the Click-iT reaction cocktail led to bleaching of EGFP; therefore, the time of staining was decreased to 10–20 min.

### Flow cytometry

EGFP–B23-expressing HeLa cells were analyzed by flow cytometry using a FACS Aria SORP instrument (BD Biosciences). The excitation laser wavelength for EGFP was 488 nm, and a combination of 505 LP and 515/20 BP filters were used for detection.

### Live-cell imaging

For live imaging experiments, cells were grown in 35-mm dishes with a coverslip (MatTek). The culture medium in the dishes was covered with mineral oil to avoid evaporation and pH changes during observation. Live imaging was performed on a Nikon A1 confocal microscope with a 60× Plan Apo objective (NA 1.4) at 37°C; focus stabilization was performed using the PFS system (Nikon).

The first step of particle tracking was compensation for global nuclear motion and deformation. Because the data were acquired in a single channel for both the objects of interest and the nucleus body, compensation was performed using a non-rigid contour-based approach (Sorokin et al., 2014). Nuclear segmentation, which is required for global motion compensation, was performed independently for each frame using the following approach: the image was denoised with a Gaussian filter, and p-tile or triangle thresholding was subsequently applied. The resulting segmentation mask was postprocessed with morphological operations (closing and hole-filling), using appropriate parameters depending on the image sequence.

For iPNB detection, we used a Hessian-based approach (Foltánková et al., 2013). The iPNB centroids were considered to be at their spatial position. Particle linking was performed using the MHT approach (Chenouard et al., 2013). Only the trajectories of the iPNBs that were stably detected throughout the entire image sequence were retained for the analysis.

For 4D microscopy, an LSM510 confocal laser scanning microscope (Carl Zeiss) was employed. Cells were maintained at 37°C using both a lens heater (Bioptech) and a stage heater (Carl Zeiss).

### Fluorescence recovery after photobleaching

For the FRAP experiments, the cells were grown in 35-mm glass-bottom Petri dishes (MatTek). The medium was overlaid with mineral oil before the experiment, and the dishes were mounted onto a Nikon A1 confocal microscope. Four single scans were acquired for the FRAP experiments, followed by a single pulse for photobleaching. The recovery curves were generated from background-subtracted images. The relative fluorescence intensity (RFI) was calculated as $RFI=T_0I_t/T_tI_0$, where $T_0$ is the total cellular intensity during prebleaching; $T_t$ is the total cellular intensity at time point t; $I_0$ is the average intensity in the region of interest during prebleaching; and $I_t$ is the average intensity in the region of interest at time point t.

### Fluorescent *in situ* hybridization

FISH was performed as described by Shishova et al. (2011). The probes were as described by Carron et al. (2012). The oligonucleotides used for FISH were labeled with 5-carboxy-X-rhodamine (Syntol). The preparations were observed with an Axiovert 200M microscope (Carl Zeiss) equipped with an Apochromat 100×1.4 NA oil immersion objective. Images were

recorded using an ORCAII-ERG2 cooled CCD camera (Hamamatsu). For brightness and contrast correction, and final presentation, all images were transferred into Adobe Photoshop (Adobe Systems).

### shRNA-mediated B23 depletion

The shRNA probe for B23 depletion was as described by Liu et al. (2007); the anti-parallel sequence was used as a control. The construction of shRNA-coding plasmids was as described elsewhere (Musinova et al., 2015). These constructs were packaged into pseudoviral particles using the pPACKH1 Lentivector Packaging Kit (System Biosciences) and transduced into HeLa cells. The transduced cells were cloned by the limiting dilution method. The B23 content in clones was determined by immunoblotting and immunocytochemistry.

#### Acknowledgements

We are grateful to Dr X. W. Wang (Center for Cancer Research, National Cancer Institute/NIH, USA) for the EGFP–B23-expressing plasmid. We thank M. Y. Mogilnikov for providing technical support and I. A. Vorobjev, K. V. Shishova, S. E. Dmitriev and P. Roussel for making valuable suggestions. We thank S. A. Golyshev for drawing the pre-rRNA processing pathways in Fig. 5.

#### Competing interests

The authors declare no competing or financial interests.

#### Author contributions

Y.R.M., O.M.L., E.A.A., T.A.S., R.A.Z., D.M.P., and E.V.S. carried out experiments, D.V.S. performed image analysis. D.V.S., Y.S.V. and E.V.S. wrote the manuscript. All authors read and approved the final manuscript.

#### Funding

This work was supported by the Russian Science Foundation (grant 14-15-00199 to E.V.S.), particle tracking and trajectory analysis were carried out using support from the Grantová Agentura České Republiky (Grant Agency of the Czech Republic) (project GBP302/12/G157 to D.V.S.), flow cytometry analysis was supported in part by M. V. Lomonosov Moscow State University Program of Development. FRAP was performed at User Facilities Centre of M. V. Lomonosov Moscow State University under financial support of Ministry of Education and Science of the Russian Federation and the Russian Foundation for Basic Research (grants 14-04-01650 and 16-54-16001 to Y.R.M.).

#### Supplementary information

Supplementary information available online at http://jcs.biologists.org/lookup/doi/10.1242/jcs.189142.supplemental

#### References

**Ahn, J.-Y., Liu, X., Cheng, D., Peng, J., Chan, P.-K., Wade, P. A. and Ye, K.** (2005). Nucleophosmin/B23, a nuclear PI(3,4,5)P(3) receptor, mediates the antiapoptotic actions of NGF by inhibiting CAD. *Mol. Cell* **18**, 435-445.

**Amin, M. A., Matsunaga, S., Uchiyama, S. and Fukui, K.** (2008). Nucleophosmin is required for chromosome congression, proper mitotic spindle formation, and kinetochore-microtubule attachment in HeLa cells. *FEBS Lett.* **582**, 3839-3844.

**Andersen, J. S., Lam, Y. W., Leung, A. K. L., Ong, S.-E., Lyon, C. E., Lamond, A. I. and Mann, M.** (2005). Nucleolar proteome dynamics. *Nature* **433**, 77-83.

**Audas, T. E., Jacob, M. D. and Lee, S.** (2012). Immobilization of proteins in the nucleolus by ribosomal intergenic spacer noncoding RNA. *Mol. Cell* **45**, 147-157.

**Avitabile, D., Bailey, B., Cottage, C. T., Sundararaman, B., Joyo, A., McGregor, M., Gude, N., Truffa, S., Zarrabi, A., Konstandin, M. et al.** (2011). Nucleolar stress is an early response to myocardial damage involving nucleolar proteins nucleostemin and nucleophosmin. *Proc. Natl. Acad. Sci. USA* **108**, 6145-6150.

**Berry, J., Weber, S. C., Vaidya, N., Haataja, M. and Brangwynne, C. P.** (2015). RNA transcription modulates phase transition-driven nuclear body assembly. *Proc. Natl. Acad. Sci. USA* **112**, E5237-E5245.

**Bertwistle, D., Sugimoto, M. and Sherr, C. J.** (2004). Physical and functional interactions of the Arf tumor suppressor protein with nucleophosmin/B23. *Mol. Cell. Biol.* **24**, 985-996.

**Bhattacharya, D., Mazumder, A., Miriam, S. A. and Shivashankar, G. V.** (2006). EGFP-tagged core and linker histones diffuse via distinct mechanisms within living cells. *Biophys. J.* **91**, 2326-2336.

**Box, J. K., Paquet, N., Adams, M. N., Boucher, D., Bolderson, E., O'Byrne, K. J. and Richard, D. J.** (2016). Nucleophosmin: from structure and function to disease development. *BMC Mol. Biol.* **17**, 19.

**Carron, C., Balor, S., Delavoie, F., Plisson-Chastang, C., Faubladier, M., Gleizes, P.-E. and O'Donohue, M.-F.** (2012). Post-mitotic dynamics of pre-nucleolar bodies is driven by pre-rRNA processing. *J. Cell Sci.* **125**, 4532-4542.

**Caudron-Herger, M., Pankert, T., Seiler, J., Németh, A., Voit, R., Grummt, I. and Rippe, K.** (2015). Alu element-containing RNAs maintain nucleolar structure and function. *EMBO J.* **34**, 2758-2774.

**Chenouard, N., Bloch, I. and Olivo-Marin, J.-C.** (2013). Multiple hypothesis tracking for cluttered biological image sequences. *IEEE Trans Pattern Anal. Mach. Intell.* **35**, 2736-3750.

**Chujo, T., Yamazaki, T. and Hirose, T.** (2015). Architectural RNAs (arcRNAs): a class of long noncoding RNAs that function as the scaffold of nuclear bodies. *Biochim. Biophys. Acta* **1859**, 139-146.

**Colombo, E., Marine, J.-C., Danovi, D., Falini, B. and Pelicci, P. G.** (2002). Nucleophosmin regulates the stability and transcriptional activity of p53. *Nat. Cell Biol.* **4**, 529-533.

**Dundr, M.** (2011). Seed and grow: a two-step model for nuclear body biogenesis. *J. Cell Biol.* **193**, 605-606.

**Dundr, M.** (2012). Nuclear bodies: multifunctional companions of the genome. *Curr. Opin. Cell Biol.* **24**, 415-422.

**Dundr, M., Misteli, T. and Olson, M. O. J.** (2000). The dynamics of postmitotic reassembly of the nucleolus. *J. Cell Biol.* **150**, 433-446.

**Foltánková, V., Matula, P., Sorokin, D., Kozubek, S. and Bártová, E.** (2013). Hybrid detectors improved time-lapse confocal microscopy of PML and 53BP1 nuclear body colocalization in DNA lesions. *Microsc. Microanal.* **19**, 360-369.

**Grob, A., Colleran, C. and McStay, B.** (2014). Construction of synthetic nucleoli in human cells reveals how a major functional nuclear domain is formed and propagated through cell division. *Genes Dev.* **28**, 220-230.

**Hennig, S., Kong, G., Mannen, T., Sadowska, A., Kobelke, S., Blythe, A., Knott, G. J., Iyer, K. S., Ho, D., Newcombe, E. A. et al.** (2015). Prion-like domains in RNA binding proteins are essential for building subnuclear paraspeckles. *J. Cell Biol.* **210**, 529-539.

**Henras, A. K., Plisson-Chastang, C., O'Donohue, M.-F., Chakraborty, A. and Gleizes, P.-E.** (2014). An overview of pre-ribosomal RNA processing in eukaryotes. *Wiley Interdiscip. Rev. RNA* **6**, 225-242.

**Hernandez-Verdun, D.** (2011). Assembly and disassembly of the nucleolus during the cell cycle. *Nucleus* **2**, 189-194.

**Hingorani, K., Szebeni, A. and Olson, M. O. J.** (2000). Mapping the functional domains of nucleolar protein B23. *J. Biol. Chem.* **275**, 24451-24457.

**Holmberg Olausson, K., Elsir, T., Moazemi Goudarzi, K., Nistér, M. and Lindström, M. S.** (2015). NPM1 histone chaperone is upregulated in glioblastoma to promote cell survival and maintain nucleolar shape. *Sci. Rep.* **5**, 16495.

**Kaiser, T. E., Intine, R. V. and Dundr, M.** (2008). De novo formation of a subnuclear body. *Science* **322**, 1713-1717.

**Koike, A., Nishikawa, H., Wu, W., Okada, Y., Venkitaraman, A. R. and Ohta, T.** (2010). Recruitment of phosphorylated NPM1 to sites of DNA damage through RNF8-dependent ubiquitin conjugates. *Cancer Res.* **70**, 6746-6756.

**Korčeková, D., Gombitová, A., Raška, I., Cmarko, D. and Lanctôt, C.** (2012). Nucleologenesis in the Caenorhabditis elegans embryo. *PLoS ONE* **7**, e40290.

**Kressler, D., Hurt, E. and Bassler, J.** (2010). Driving ribosome assembly. *Biochim. Biophys. Acta* **1803**, 673-683.

**Kurki, S., Peltonen, K., Latonen, L., Kiviharju, T. M., Ojala, P. M., Meek, D. and Laiho, M.** (2004). Nucleolar protein NPM interacts with HDM2 and protects tumor suppressor protein p53 from HDM2-mediated degradation. *Cancer Cell* **5**, 465-475.

**Lee, S. Y., Park, J.-H., Kim, S., Park, E.-J., Yun, Y. and Kwon, J.** (2005). A proteomics approach for the identification of nucleophosmin and heterogeneous nuclear ribonucleoprotein C1/C2 as chromatin-binding proteins in response to DNA double-strand breaks. *Biochem. J.* **388**, 7-15.

**Li, Z. and Hann, S. R.** (2009). The Myc-nucleophosmin-ARF network: a complex web unveiled. *Cell Cycle* **8**, 2703-2707.

**Lindström, M. S.** (2011). NPM1/B23: a multifunctional chaperone in ribosome biogenesis and chromatin remodeling. *Biochem. Res. Int.* **2011**, 195209.

**Liu, H., Tan, B. C.-M., Tseng, K. H., Chuang, C. P., Yeh, C.-W., Chen, K.-D., Lee, S.-C. and Yung, B. Y.-M.** (2007). Nucleophosmin acts as a novel AP2alpha-binding transcriptional corepressor during cell differentiation. *EMBO Rep.* **8**, 394-400.

**Mao, Y. S., Zhang, B. and Spector, D. L.** (2011a). Biogenesis and function of nuclear bodies. *Trends Genet.* **27**, 295-306.

**Mao, Y. S., Sunwoo, H., Zhang, B. and Spector, D. L.** (2011b). Direct visualization of the co-transcriptional assembly of a nuclear body by noncoding RNAs. *Nat. Cell Biol.* **13**, 95-101.

**Misteli, T.** (2001). The concept of self-organization in cellular architecture. *J. Cell Biol.* **155**, 181-186.

**Mitrea, D. M., Grace, C. R., Buljan, M., Yun, M.-K., Pytel, N. J., Satumba, J., Nourse, A., Park, C.-G., Madan Babu, M., White, S. W. et al.** (2014). Structural polymorphism in the N-terminal oligomerization domain of NPM1. *Proc. Natl. Acad. Sci. USA* **111**, 4466-4471.

**Muro, E., Gébrane-Younès, J., Jobart-Malfait, A., Louvet, E., Roussel, P. and Hernandez-Verdun, D.** (2010). The traffic of proteins between nucleolar organizer regions and prenucleolar bodies governs the assembly of the nucleolus at exit of mitosis. *Nucleus* **1**, 202-211.

**Musinova, Y. R., Kananykhina, E. Y., Potashnikova, D. M., Lisitsyna, O. M. and Sheval, E. V.** (2015). A charge-dependent mechanism is responsible for the

dynamic accumulation of proteins inside nucleoli. *Biochim. Biophys. Acta* **1853**, 101-110.

**Nott, T. J., Petsalaki, E., Farber, P., Jervis, D., Fussner, E., Plochowietz, A., Craggs, T. D., Bazett-Jones, D. P., Pawson, T., Forman-Kay, J. D. et al.** (2015). Phase transition of a disordered nuage protein generates environmentally responsive membraneless organelles. *Mol. Cell* **57**, 936-947.

**Prasanth, K. V., Sacco-Bubulya, P. A., Prasanth, S. G. and Spector, D. L.** (2003). Sequential entry of components of gene expression machinery into daughter nuclei. *Mol. Biol. Cell* **14**, 1043-1057.

**Rajendra, T. K., Praveen, K. and Matera, A. G.** (2010). Genetic analysis of nuclear bodies: from nondeterministic chaos to deterministic order. *Cold Spring Harb. Symp. Quant. Biol.* **75**, 365-374.

**Salzler, H. R., Tatomer, D. C., Malek, P. Y., McDaniel, S. L., Orlando, A. N., Marzluff, W. F. and Duronio, R. J.** (2013). A sequence in the Drosophila H3-H4 Promoter triggers histone locus body assembly and biosynthesis of replication-coupled histone mRNAs. *Dev. Cell* **24**, 623-634.

**Savino, T. M., Gébrane-Younès, J., De Mey, J., Sibarita, J.-B. and Hernandez-Verdun, D.** (2001). Nucleolar assembly of the rRNA processing machinery in living cells. *J. Cell Biol.* **153**, 1097-1110.

**Shav-Tal, Y., Blechman, J., Darzacq, X., Montagna, C., Dye, B. T., Patton, J. G., Singer, R. H. and Zipori, D.** (2005). Dynamic sorting of nuclear components into distinct nucleolar caps during transcriptional inhibition. *Mol. Biol. Cell* **16**, 2395-2413.

**Sheval, E. V., Polzikov, M. A., Olson, M. O. J. and Zatsepina, O. V.** (2005). A higher concentration of an antigen within the nucleolus may prevent its proper recognition by specific antibodies. *Eur. J. Histochem.* **49**, 117-123.

**Shevtsov, S. P. and Dundr, M.** (2011). Nucleation of nuclear bodies by RNA. *Nat. Cell Biol.* **13**, 167-173.

**Shishova, K. V., Zharskaya, C. O. and Zatsepina, O. V.** (2011). The fate of the nucleolus during mitosis: comparative analysis of localization of some forms of pre-rRNA by fluorescent in situ hybridization in NIH/3T3 mouse fibroblasts. *Acta Naturae* **3**, 100-106.

**Sirri, V., Jourdan, N., Hernandez-Verdun, D. and Roussel, P.** (2016). Sharing the mitotic pre-ribosomal particle between daughter cells. *J. Cell Sci.* **129**, 1592-1604.

**Sleeman, J. E. and Trinkle-Mulcahy, L.** (2014). Nuclear bodies: new insights into assembly/dynamics and disease relevance. *Curr. Opin. Cell Biol.* **28**, 76-83.

**Sorokin, D. V., Tektonidis, M., Rohr, K. and Matula, P.** (2014). Non-rigid contour-based temporal registration of 2D cell nuclei images using the Navier equation. In 2014 IEEE 11th International Symposium on Biomedical Imaging (ISBI), 746-749.

**Spille, J.-H., Kaminski, T. P., Scherer, K., Rinne, J. S., Heckel, A. and Kubitscheck, U.** (2015). Direct observation of mobility state transitions in RNA trajectories by sensitive single molecule feedback tracking. *Nucleic Acids Res.* **43**, e14.

**Svistunova, D. M., Musinova, Y. R., Polyakov, V. Y. and Sheval, E. V.** (2012). A simple method for the immunocytochemical detection of proteins inside nuclear structures that are inaccessible to specific antibodies. *J. Histochem. Cytochem.* **60**, 152-158.

**Wang, D., Baumann, A., Szebeni, A. and Olson, M. O.** (1994). The nucleic acid binding activity of nucleolar protein B23.1 resides in its carboxyl-terminal end. *J. Biol. Chem.* **269**, 30994-30998.

**Wang, W., Budhu, A., Forgues, M. and Wang, X. W.** (2005). Temporal and spatial control of nucleophosmin by the Ran-Crm1 complex in centrosome duplication. *Nat. Cell Biol.* **7**, 823-830.

**Weber, S. C. and Brangwynne, C. P.** (2015). Inverse size scaling of the nucleolus by a concentration-dependent phase transition. *Curr. Biol.* **25**, 641-646.

**White, A. E., Burch, B. D., Yang, X.-C., Gasdaska, P. Y., Dominski, Z., Marzluff, W. F. and Duronio, R. J.** (2011). Drosophila histone locus bodies form by hierarchical recruitment of components. *J. Cell Biol.* **193**, 677-694.

**Zatsepina, O. V., Dudnic, O. A., Todorov, I. T., Thiry, M., Spring, H. and Trendelenburg, M. F.** (1997). Experimental induction of prenucleolar bodies (PNBs) in interphase cells: interphase PNBs show similar characteristics as those typically observed at telophase of mitosis in untreated cells. *Chromosoma* **105**, 418-430.